Original Study   **Open Access**

Hubert Szabowicz*, Marek Kawa, Wojciech Puła

Efficient and conservative estimation reliability analysis of strip footing on spatially variable c - ϕ soil using random finite element limit analysis

Abstract: The study deals with reliability analysis of strip foundation on spatially variable c - ϕ soil. The spatial variability of soil strength parameters, namely cohesion c and friction angle ϕ is modelled using anisotropic uncorrelated random fields, generated with the Fourier series method. Random finite element limit analysis (RFELA) providing a rigorous lower and upper bound for bearing capacity for individual Monte-Carlo simulations is employed. Additional use of adaptive meshing refinement algorithm leads to a significant reduction of the relative difference between statistical moments of obtained lower and upper bound results. The influence of the horizontal and vertical scales of fluctuation and foundation depths on the mean and standard deviation of the obtained bound moments is investigated. Additionally, the rigorousness of the mean and standard deviation of both considered bounds estimation is checked. As a result of the analysis, a novel approach based on a mixed distribution that combines lower and upper bound moments is introduced. As shown, this approach offers significant benefits by providing conservative and relatively precise measures of reliability which can be obtained in reasonable computation time. The proposed method seems to be adequate for practical engineering reliability analysis of foundation bearing capacity and other limits states problems.

Keywords: Strip Fundation; Random field; Random Finite Element Limit Analysis; Reliability Analysis.

1 Introduction

Geotechnical structures, particularly the foundations, are an important part of the civil engineering discipline. Embedded in soil or built at the surface level, they form the base for the rest of the structure, which means that their potential failure usually leads to the failure of other structural elements (Kawa, 2023; Kawa & Puła, 2020). Meanwhile, the soil surrounding the foundation is often highly spatially variable (Ching et al., 2018). Due to limited budgets, its parameters can only be investigated at selected locations (Jerez et al., 2024). As a result, the design of geotechnical structures is often associated with greater uncertainty and their failure with greater consequences than other branches of civil engineering. It is therefore not surprising that the field of structural reliability, which has developed strongly in recent decades, is particularly concerned with geotechnical structures, indicating that the principal source of uncertainty for them is the spatial variability of the soil parameters.

The reliability of the foundations can be analysed. In such analysis, it is possible to take into account the spatial variability of soil parameters, e.g., using stationary random fields (J. L. Doob, 1990), which according to many works (e.g., Hicks & Samy, 2002; Griffiths et al., 2009; Pieczyńska-Kozłowska et al., 2015) should be considered as anisotropic. Identification of such field consists of two parts: identification of probability distribution of parameters and identification of so-called autocorrelation function or more precisely its parameters, scales of fluctuation (SOFs), separately in the horizontal and vertical direction. The latter quantities can be simply understood as average dimensions of the random cluster in the field within which the values of the given parameter are strongly correlated. Application of random fields for the description of soil parameters is indicated as an appropriate approach by, i.e. annexe D of the newest edition of the ISO 2394:2015 code dedicated to reliability analysis.

*Corresponding author: Hubert Szabowicz, Faculty of Civil Engineering, Wroclaw University of Science and Technology, Wyb. Wyspianskiego 27, 50-370 Wroclaw, Poland, E-mail: hubert.szabowicz@pwr.edu.pl
Marek Kawa, Wojciech Puła, Faculty of Civil Engineering, Wroclaw University of Science and Technology, Wyb. Wyspianskiego 27, 50-370 Wroclaw, Poland

A popular and universal method that employs random fields to describe crucial soil parameters for numerical calculations is the random finite element method (RFEM) (Griffiths & Fenton, 1993; Fenton & Griffiths, 2008). It consists of sequential mapping of random field values for many realisations to the part of the finite element (FE) mesh, representing the soil medium in a numerical problem model. The probabilistic results are based on a statistical analysis of considered structure responses taken from all the mapped realisations, each computed as an individual Monte-Carlo simulation (MCS). The method enables probabilistic modelling of any virtually geotechnical structure which can be modelled with FE by either linear or nonlinear models. Until now, the method was used to analyse different types of foundations (e.g., Fenton & Griffiths, 2008; Kawa & Puła, 2020; Dobrzanski & Kawa, 2021; Chen et al., 2022; Kumar et al., 2023), but also other geotechnical structures such as slopes (e.g., Griffiths & Fenton, 2004; Huang et al., 2021), diaphragm walls (Sert et al., 2016; Kawa et al., 2021), piles (Cheng et al., 2023), etc. The greatest disadvantage of the RFEM lies in its significantly high computation cost being a direct result of the computation cost of a single MCS. Given the typical number of N=1000 MCSs (which in the case of the ultimate limit state allows only for a rough estimation of failure probability, cf. Kawa et al., 2021) and the typical range of time needed to solve a problem realisation (dependent on the complexity of the problem), the total computation time on a modern PC is usually between few hours and several days. Such a long time significantly limits the possibility of using the method in engineering practice. For this reason, more efficient alternatives, which are based on the quasi-analytical kinematic method (e.g., Chwała, 2019) or limit equilibrium method (e.g., Liu et al., 2019) are still being sought.

One of the alternatives to RFEM is random finite element limit analysis (RFELA), a more efficient approach, which is also based on mapping random field realisations into a discretised domain. It is a modification of RFEM, which uses finite element limit analysis (FELA, Lyamin & Sloan, 2002a, 2002b) instead of the typical FE method (FEM) to solve individual simulations. The class of the problem is limited here to limit states. For such problems, FELA enables the rigorous determination of both the lower (based on the static approach) and the upper (based on the kinematic approach) bounds (LBs, UBs) of the solution (e.g., bearing capacity value) by solving constrained convex optimisation problems, which is a much faster approach than traditional elastic-perfectly plastic FEM analyses. With the additional use of adaptive meshing refinement, these bounds, in successive iterations, can quite precisely estimate the exact solution (their relative difference can be less than 2%). Adaptive and nonadaptive algorithms of RFELA have been used mostly for probabilistic assessment of foundations bearing capacity (e.g., Simões et al., 2014; Ali et al., 2016) and factors of stability for slopes until now (Ali et al., 2017), however, the list of problems analysed is constantly expanding. Recently, the method (implemented in commercial code OPTUM 2G) was, e.g., used to estimate the average diameter of randomly irregular lunar lava tubes (Chwała et al., 2024). Although the cited and similar works take advantage of the high speed of the RFELA, in the authors' opinion, the rigorousness of the LBs and UBs so far has not been fully utilised.

This paper attempts to exploit both advantages of the RFELA method, i.e., high speed and rigorousness of bounds estimation. Both approaches can be utilised to estimate the mean and standard deviation of the UB and LB, respectively. The efficiency of the algorithm enabled quick and accurate estimation of these moments using a limited number of adaptive mesh refinements. The estimated moments were used to define the mixed distribution, i.e., one obtained by assuming mean based on a static approach and standard deviation based on a kinematic approach. As shown, the results of the novel approach can be used for quick, conservative and relatively precise reliability analysis.

The subject of this study is an analysis of the bearing capacity of strip foundations on c - φ soil. Both friction and cohesion are modelled by anisotropic random fields generated with the Fourier series method (FSM, Jha & Ching, 2013). Three foundation levels and several different values of the horizontal and vertical scales of fluctuation were analysed. The LBs and UBs of bearing capacity in individual realisations are determined using FELA formulations proposed by Lyamin and Sloan (2002a) and Makrodimopoulos and Martin (2008), respectively. These formulations were implemented by the authors in Matlab code. In each realisation, the solutions for the LBs and UBs were obtained using the commercial solver MOSEK. The influence of both horizontal and vertical fluctuation scales and foundation levels on the probabilistic characteristics of bearing capacity assessments was investigated. As shown, the applied numerical algorithm allowed for quite precise and rigorous estimation of mean and variance in both approaches. Additional use of the mentioned mixed distribution enabled conservative and precise estimation of allowable load value satisfying given failure probability condition.

2 Methodology

2.1 Random field generation

The assumed soil is of c - φ type. Both soil strength parameters were described with random fields. It is assumed that these fields are stationary and anisotropic. Since c and φ are usually reported as negatively correlated and such correlation typically results in a lower standard deviation of bearing capacity (cf. Cho & Park 2010) and consequently lower probability of failure, the fields were also assumed uncorrelated for conservatism. Both probability distributions were assumed to be lognormal. To generate the random fields, the FSM was utilised. This approach approximates the autocorrelation function by applying a finite Fourier series. The value of the field at a given point in 2D space with coordinates x and z is calculated as the following double sum:

$$W(\mathbf{X}) = W(x,z) = \sum_{-m}^{m} \sum_{-n}^{n} (a_{mn} + ib_{mn}) \exp\left(i2\pi\left(\frac{m \cdot x}{L_x} + \frac{n \cdot z}{L_z}\right)\right) \quad (1)$$

where a_{mn}, b_{mn} are independent random variables with a normal distribution N(0,σ_{mn}) with σ_{mn} dependent on the chosen autocorrelation function and L_x and L_z are the dimensions of the domain over which the simulations are performed. The length of the series is determined by the numbers m and n which depend on the assumed precision and the assumed autocorrelation function. Please note that the description of the random field by a continuous function, that allows the value of the field realisation at any point to be determined independently of the element mesh, is a mandatory condition for RFELA analysis which implements the mesh adaptation procedure. The results obtained by the FELA method are strongly affected by the FE mesh fitting to the failure mechanism obtained in a given realisation. The implementation of an iterative procedure that allows the mesh shape to be adapted to the mechanism makes it possible to increase its accuracy without an excessive increase in the number of elements. A description of the mesh adaptation algorithm is provided in the later sections.

The FSM algorithm generates random fields with normal distribution. Since the distribution of soil parameters was assumed as lognormal, the fields with the parameters for the underlying normal distribution $RF_Y(X)$ were first generated. The mean value (μ_g) and standard deviation (σ_g) of the underlying normal distribution can be calculated using the analytical formulas that link these moments to moments of the target lognormal distribution {μ,σ}, namely,

$$\sigma_g^2 = \ln\left(1 + \frac{\sigma^2}{\mu^2}\right), \quad \mu_g = \ln(\mu) - \frac{1}{2}\sigma_g^2 \qquad (2)$$

After generation, the values of the underlying normal field were further transformed to lognormal field $RF_X(X)$ according to formula (2).

$$RF_X(X) = \exp(RF_Y(X)), \qquad (3)$$

where X={x,z} denotes the coordinate of the point that belongs to the random field.

Both random fields were assumed to be characterised by a Gaussian autocorrelation function according to the following formula:

$$\rho(\tau_x, \tau_z) = \exp\left\{-\pi\left[\left(\frac{\tau_x}{\theta_x}\right)^2 + \left(\frac{\tau_z}{\theta_z}\right)^2\right]\right\} \qquad (4)$$

where τ_x, τ_z are, respectively, the distance between two points on the horizontal (x) and vertical (z) axes, and θ_x, θ_z are the horizontal and vertical scales of fluctuation. The Gaussian autocorrelation function was chosen because of the low length of the associated Fourier series (compared with, e.g., exponential function) which affects the time of random filed values calculation.

2.2 Finite element limit analysis

As mentioned, the RFELA method utilises FELA to solve individual realisations of the given problem. The latter is one of the possible numerical methods capable of solving the limit state problem, e.g., of the load-bearing capacity of a shallow foundation. The method requires several assumptions to be made which significantly simplify the model while omitting the knowledge of the deformation state. On the other hand, it enables a considerable reduction in calculation time compared with, e.g., the FE or the finite difference methods. Most importantly, FELA provides rigorous lower and upper limits of bearing capacity.

The LB and UB solutions are determined, respectively, by searching for the maximum load corresponding to the statically admissible stress field and the minimum load for which the kinematically admissible displacement velocity field is developed. Both issues represent a mathematical optimisation problem. This article uses the approaches described by Lyamin and Sloan (2002a) in the context of LB estimation and Makrodimopoulos and Martin (2008) regarding UB estimation. A perfectly plastic material model with an associated flow rule is

assumed. The FE mesh consists of triangular elements for which a linear shape function is used for the stresses and a quadratic shape function is used for the displacement velocities when estimating the LB and UB, respectively. As previously mentioned, the Coulomb–Mohr material model with strength parameters c and ϕ is assumed. This model can easily be written in the form of a conic quadratic constraint, which enables finding the solution of both UB and LB using second-order cone programming. The letter appears to be a very efficient method for solving optimisation problems.

The LB and UB problems are weakly dual, which means that their solutions differ by a certain gap due to discretisation error. On the other hand, strongly dual problems with the same solutions can be formulated to each of the task (Ciria Suárez, 2004). The dual problem to the kinematic approach involves searching for an admissible stress distribution (slightly different from the one in static approach), while the dual problem to the static approach involves searching for an admissible failure mechanism (slightly different from the one in kinematic approach). In this article, both problems are formulated by searching for the stress distribution (i.e., the original static problem and the dual to kinematic problem are solved), because, as noted by Krabbenhoft et al. (2005), a dual problem to the kinematic approach could be easier to solve.

Both mentioned problems can be described by the following equations provided by Podlich (2018):

$$\text{maximise:}$$
$$\alpha$$
$$\text{subject to:} \tag{5}$$
$$B^T \sigma = \alpha p + p_0$$
$$f(\sigma^e) \leq_K 0 \ \forall \ e=1,2,...,n_e$$

where α is the searched load value multiplier and σ is the global stress vector different for LB and UB analysis. Additionally, B^T contains the coefficients of the static equilibrium equations significantly different for the LB and UB limit analysis. Vectors p and p_0 contain the optimised and permanent load. In both cases, the Coulomb–Mohr plasticity condition is defined for all elements in the form of SOCP (Second Order Cone Programming).

On the other hand, in both approaches, the mesh adaptation algorithm utilises parameters of plastic multipliers, which are obtained by solving duals to the mentioned problems. To solve the problems, the commercial software MOSEK run from the Matlab environment was used. According to the knowledge of the authors of this study, this is the most effective

software currently available for solving many different types of optimisation problems (including SOC) (Podlich et al., 2014). The software uses the primal–dual method, which allows the automatic solution of a primal and dual problem, providing a full range of information on stresses, plastic multipliers and displacement velocities for both LB and UB estimates.

2.3 Mesh adaptive procedure

The degree to which the mesh is adapted to the shape of the failure mechanism has a significant impact on the results obtained from the optimisation problems. Obviously, increasing the mesh density over the entire domain will greatly reduce the difference between the LB and UB estimates, however, the number of nodes resulting from such mesh is computationally prohibited. For more efficient computations, elements should be densified in a specific manner only in the zone of interest.

For mesh generation, a tool called MESH2D (Engwirda, 2014) for the Matlab environment, which allows the generation of triangular meshes suitable for use in the FELA method, is utilised. This generator is based on the Delaunay method. It includes options to modify the meshes both by subdividing the indicated elements and requesting a density function in the form of a dimension expectations map. The mesh adaptation procedure utilised in the calculations described below assumes that the yielding elements should be subdivided. These elements are indicated based on the plasticity multipliers obtained from both the UB and LB analyses.

In the first step, the same low-density mesh is generated regardless of the realisation of the random field. Smaller elements occur only at the corners of the foundation due to the use of so-called 'element fans', which are necessary to reduce the influence of the singularity located at the specified points (Lyamin & Sloan, 2003). Performing a FELA analysis with such a generated mesh is extremely time-efficient and gives a rough indication of the potential plastic zones. In the second step, a mesh density function, which assumes minimum dimensions for the elements that have yielded and maximum dimensions for all the others, is applied. This operation enables the refinement of the areas where the plasticity multiplier is present without an excessive increase in the number of elements. In the next steps, the elements with the highest plastic multiplier values are selected and subdivided using the MESH2D tool. The limit values of the plastic multiplier are chosen depending on the individual task. The algorithm must try to match the shape of the mesh with the results
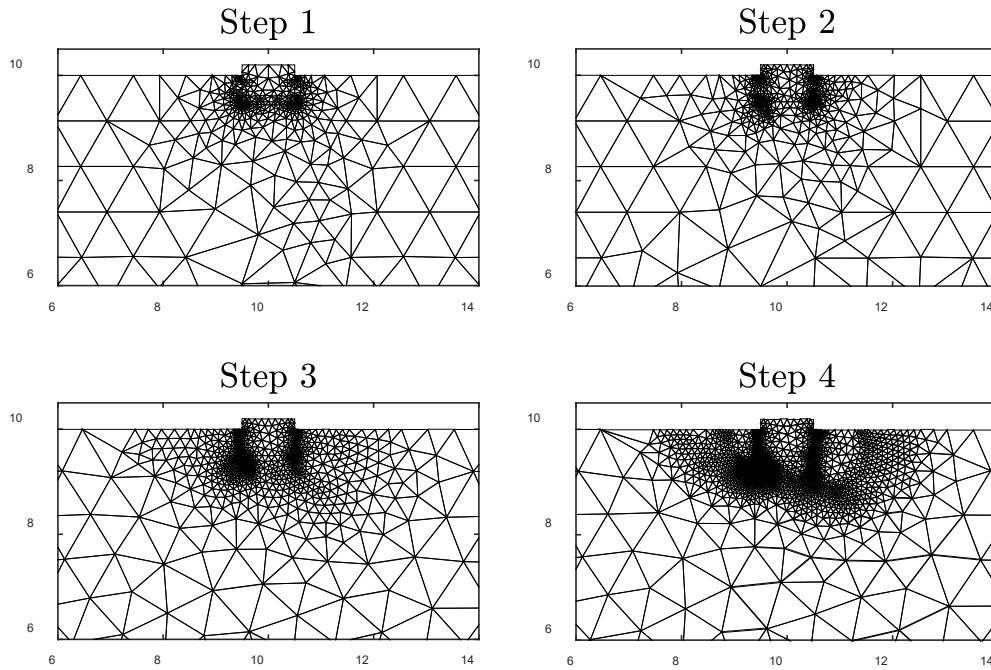
Figure 1: A graphical representation of the mesh adaptive procedure.

of both estimations. As mentioned, often the static and kinematic mechanisms may differ. The algorithm applied in the current work consists of four steps. A graphical representation of the discussed algorithm for a zoomed area around the foundation is illustrated in Figure 1.

2.4 Numerical model analysed with FELA

The study investigates the effect of the foundation depth and the value of vertical and horizontal scales of fluctuation on the bearing capacity of a shallow foundation placed on spatially variable soil. The first analysis results for a slightly different formulation of the FELA algorithm and a different mesh adaptive procedure were presented by Puła et al. (2022). The deliberation was limited to the shallow foundation with D=0.0 m only. A full analysis was carried out in the present work.

The foundation was assumed as a rigid body with a load uniformly distributed over the top face. It was allowed to rotate if such movement resulted from an optimal failure mechanism. Boundary conditions were adopted as indicated in Figure 2. The width and height of the model were assumed to be 20.0 m and 10.0 m, respectively, which allowed to ensure that no failure mechanism reached the area boundary. The width of the foundation was 1.0 m. Three foundation depth scenarios with D=0.0 (foundation placed on the ground surface), 0.5 and 1.0 m were

considered. The surface model is a frequently adopted theoretical model. On the other hand, the typical direct foundation depth oscillates around 1.0 m. A value of half a metre was assumed as an intermediate value to present a potentially nonlinear influence of embedded depth. It was assumed that the foundation established at a depth greater than zero is a rigid body that extended above the ground surface (no backfill soil overlying the foundation was assumed). Please note that the foundation material was assumed as infinitely strong (conditions of the Mohr–Coulomb criterion were not checked within the foundation).

For each foundation level, a set of five horizontal fluctuation scales θ_x={1.0,2.0,4.0,8.0,16.0 m} and a set of three vertical scales θ_z={0.25,0.5,1.0 m} were considered. The analyses included pairs formed from all possible combinations of these values. The values of cohesion (μ_c,σ_c) and internal friction angle $(\mu_\varphi,\sigma_\varphi)$ were described by the random fields realisation generated for these values as described earlier. The parameters of the lognormal distribution assumed for generation for both fields were assumed as μ_c=29.0kPa, σ_c=7.0 kPa for cohesion and μ_φ=12.41°, σ_φ=1.15° for friction angle. The soil weight was assumed to be 20 kN/m³. The specified parameters were adapted after Zaskórski and Puła (2016), who utilised them in their investigations of clay soil layers. Probabilistic analysis was carried out using the Monte-Carlo method. For each problem (each assumed
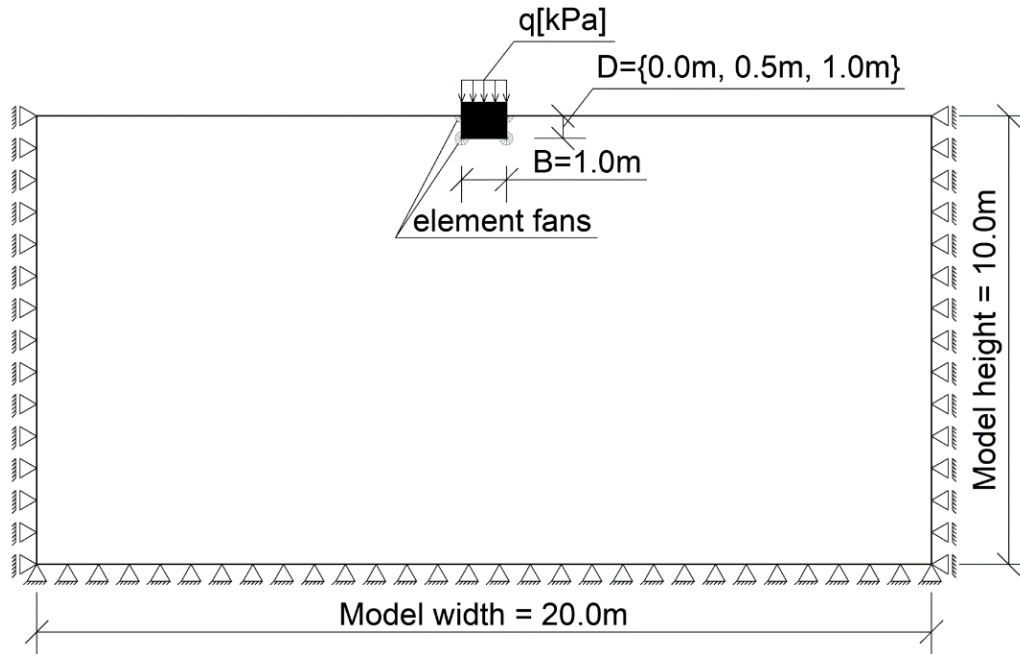
Figure 2: Model geometry with boundary condition.

pair of scales of fluctuation), 10,000 MCS was solved. The LB and UB estimates of bearing capacity were obtained for each problem realisation. A summary of the results obtained for all considered vertical and horizontal scales of fluctuations and foundation levels is reported in the following section.

3 Results

As a result of the performed analyses, the values of the LBs and UBs of bearing capacity from 10,000 MCS for each of the three considered foundation levels and 15 pairs of fluctuation scales, were obtained. Only selected results are presented in the following subsections. It is generally known that the vertical scale of fluctuation is considerably simpler to determine due to the greater number of data recorded in the vertical direction during, e.g., CPTu tests. Typically, the horizontal scale of fluctuations is quite challenging to identify because of the considerable distance between sounding points. (cf. Ching et al., 2018). For more distanced CPTu tests, this fact can lead to a situation where the vertical scale of fluctuation is known and the horizontal scale of fluctuation is unknown and is, e.g., a subject of parameter study. Analysis with such assumption was performed in some of the authors' previous work (Kawa et al. 2019, 2021). A similar assumption for presenting the result was assumed here. For this reason on the single graph, results obtained for

fixed vertical scale and changing horizontal fluctuation scale are presented rather, than otherwise.

First, the improvement in convergence of the obtained LB and UB results for bearing capacity with each subsequent adaptive mesh refinement step was analysed. All results were computed for a fixed vertical fluctuation scale of $\theta_z=1$ m with various values of the horizontal fluctuation scale, as shown in Figures 3, 4 and 5. The results for foundation depths of D = 0.0, 0.5 and 1.0 m are presented in Figures 3, 4, and 5, respectively. In each case, the data are given in the form of histograms and graphs of the estimated probability density functions, which are assumed to be lognormal. The blue lines represent the results of the LB limit analysis, while the red lines represent the results of the UB limit analysis. In individual columns, the outcomes for the different values of the horizontal scales of fluctuation, namely $\theta_x=\{1.0, 2.0, 4.0, 8.0, 16.0$ m$\}$. The results obtained at each step of the mesh adaptive procedure are provided in separate rows, with the final results being shown in the last row.

It can be observed that, for each case analysed, the mesh adaptive procedure fulfils its purpose by significantly reducing the gap between the distributions of the LB and UB estimations. After four steps of adaptation, the distributions agree almost ideally. In addition, the character of the changes caused by varying the value of fluctuation scales is very similar regardless of the assumed foundation level, namely, the histograms obtained for the subsequent horizontal scales of fluctuation oscillate
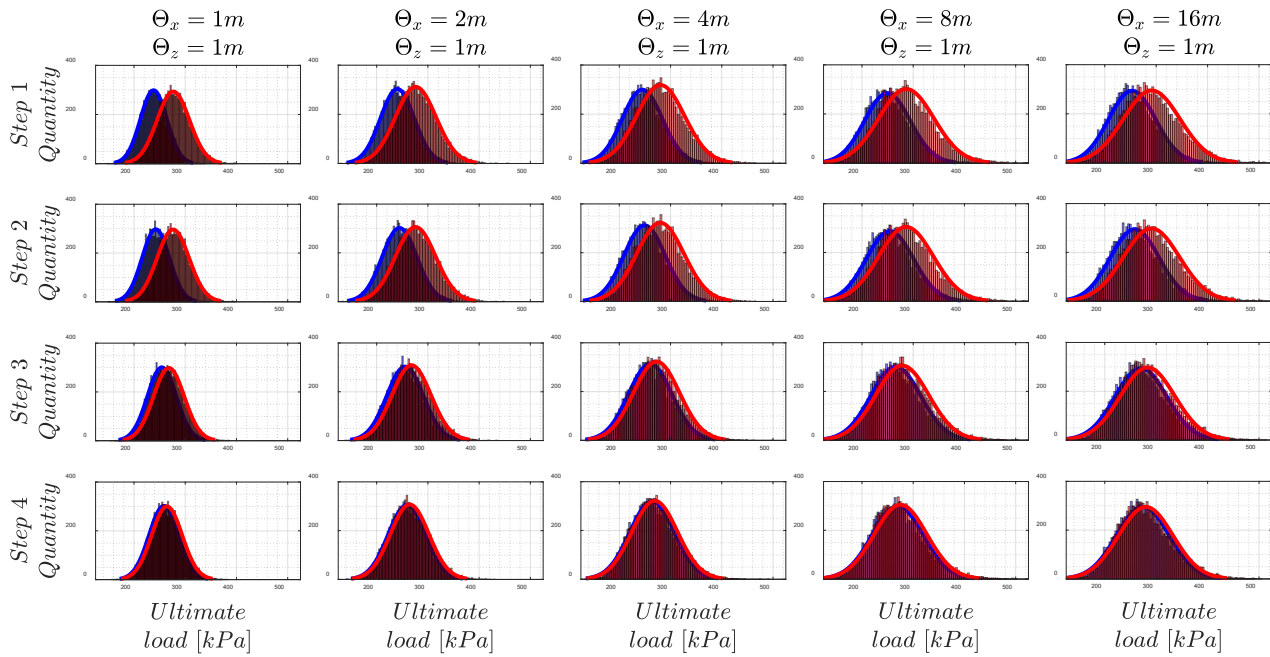
Figure 3: Upper (red lines) and lower (blue lines) bound of bearing capacities of a shallow foundation *D*=0.0 m.

around the same mean values, while simultaneously being characterised by greater values of standard deviations. As the results obtained for other analysed vertical scales of fluctuation are qualitatively very similar, they were not presented in this form.

In Figures 6–8, the convergence of mean values, standard deviations and coefficients of variation of LBs μ_{LB}, σ_{LB}, ν_{LB} and LBs μ_{UB}, σ_{UB}, ν_{UB} of bearing capacity calculated for obtained series of results are presented as a function of the mesh adaptive procedure step. In the individual drawing, the results obtained for different values of vertical fluctuation scale namely θ_z={1.0,0.5,0.25 m} are presented. Similar to the previous illustrations, results for different horizontal scales of fluctuation are presented in individual columns. Again, the blue colour indicates the LB and the red colour the UB of bearing capacity. The results corresponding to different foundation levels, *D*=0.0, 0.5 and 1.0 m, are marked with continuous, dashed and dotted lines, respectively. As observed, although the value and rate of convergence depend on the specific case of foundation depth or fluctuation scale, in each scenario, both moments exhibit lower values for the LB estimation and higher values for the UB estimation. While this behaviour is intuitive for the mean values, it is less so for the standard deviation. Additionally, since the rate of convergence can differ between the mean and standard deviation, this behaviour does not extend to the coefficient of variation.

In most of the instances, the values of the coefficient of variation may unexpectedly change their relative order during the convergence process.

Figure 9 illustrates the estimation relative difference between the upper and lower approach in the mean, standard deviation and coefficient of variation as a function of the step of the mesh adaptive procedure. The results corresponding to different foundation levels are presented in different columns. The advantage of applying an algorithm that adapts the mesh topography to the failure mechanism is clearly visible in this figure. For the mean value, the differences between the lower and upper estimates for the initial calculations with sparse mesh are in the range of 15.0%–23.5% and then, in the last step of mesh adaption, fall to the range 2.0%–6.1% for the foundation level *D*=0.0 m, 2.7%–7.2% for *D*=0.5 m and 3.2%–8.6% for *D*=1.0 m. The analogous behaviour can be observed for the relative differences in standard deviation estimation. The algorithm reduces the error from 19.7% to 37.2% for the initial meshing to, respectively, 3.0%–12.3% for *D*=0.0 m, 3.2%–7.5% for *D*=0.5 m and 2.1%–5.0% for *D*=1.0 m in the final calculation step. Once again, differing rates of convergence for the mean and standard deviation lead to unexpected behaviour in the coefficient of variation. In some cases, the relative difference in this statistic can be higher in the final step than in the preceding one. Moreover, for greater depths, negative values of the relative difference may occur indicating that
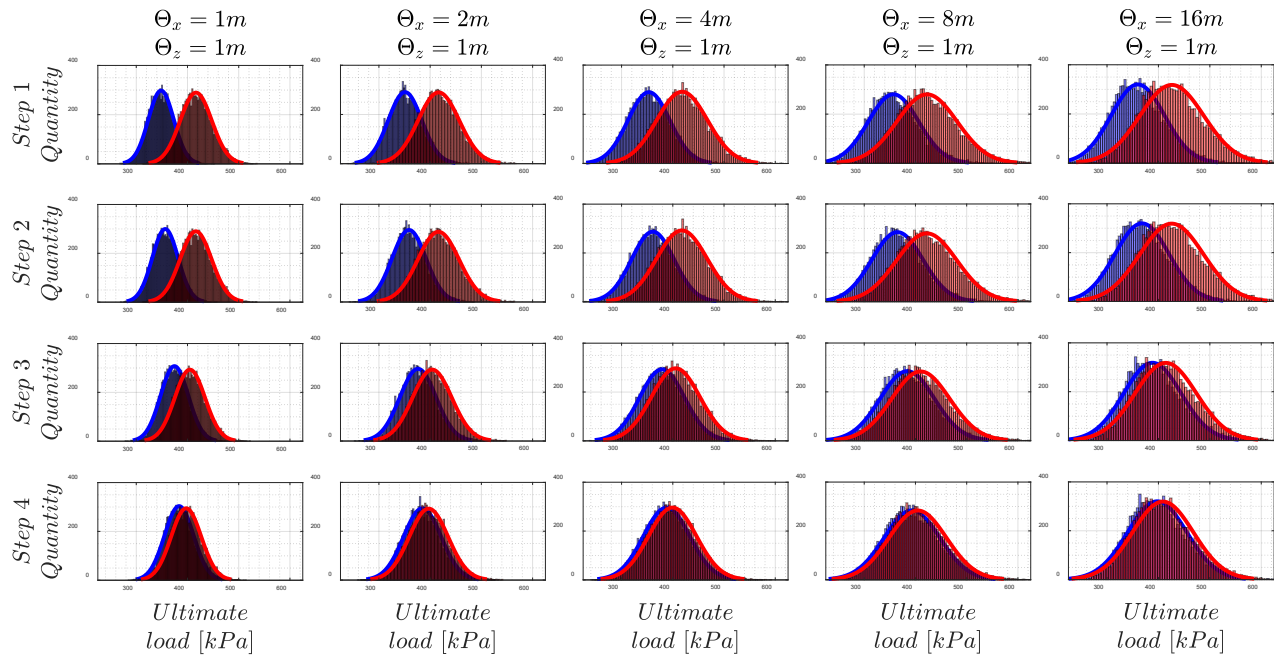
Figure 4: Upper (red lines) and lower (blue lines) bound of bearing capacities of a shallow foundation *D*=0.5 m.
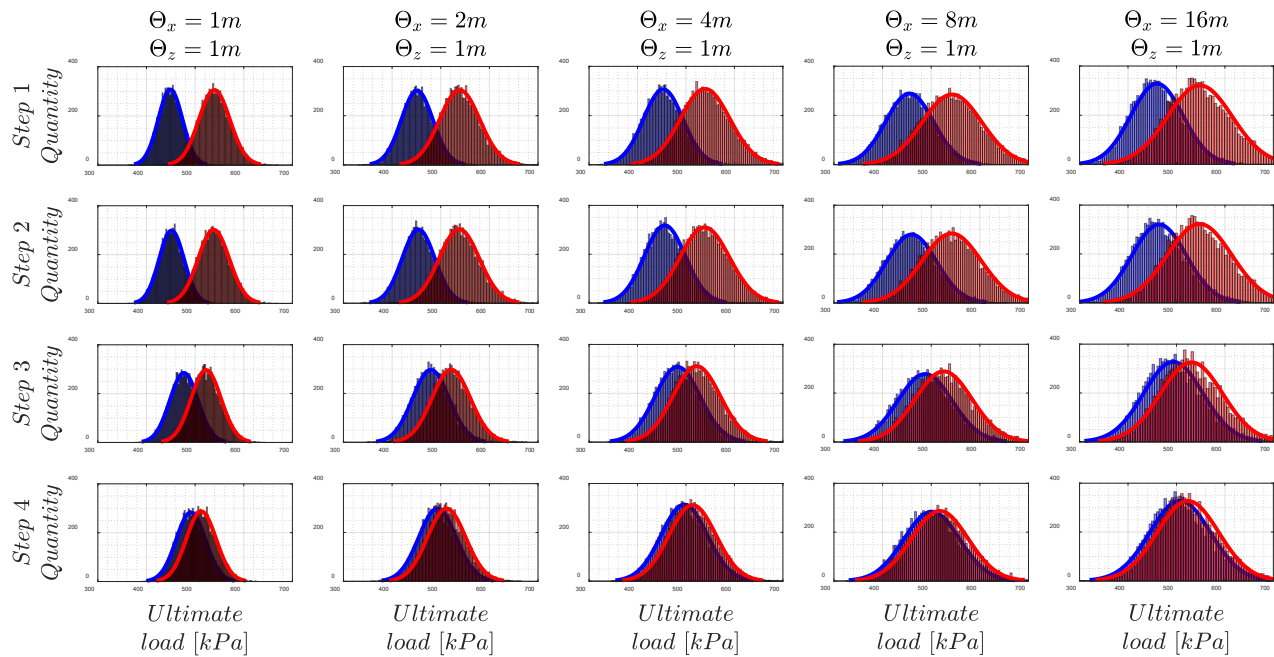

Figure 5: Upper (red lines) and lower (blue lines) bound of bearing capacities of a shallow foundation *D*=1.0 m.

the coefficient of variation is higher for the LB results than for the UB results.

The mean values, standard deviations and coefficients of variation for the last step of the mesh adaptive procedure as a function of the horizontal scale of fluctuation have been presented in Figure 10. Once

again, the LB estimations are indicated by blue and the UB estimations by red lines. In individual columns, the results for each foundation depth are presented.

The results presented in Figure 10 confirm the previous observations. The mean values seem to be practically independent of the value of the horizontal fluctuation

Figure 6: Diagrams of mean value, standard deviation and coefficient of variation of bearing capacities of a shallow foundation as a function of the step of adaptive mesh refinement procedure for vertical scale of fluctuation θ_z=0.25 m.

Figure 7: Diagrams of mean value, standard deviation and coefficient of variation of bearing capacities of a shallow foundation as a function of the step of adaptive mesh refinement procedure for vertical scale of fluctuation θ_z=0.5 m.
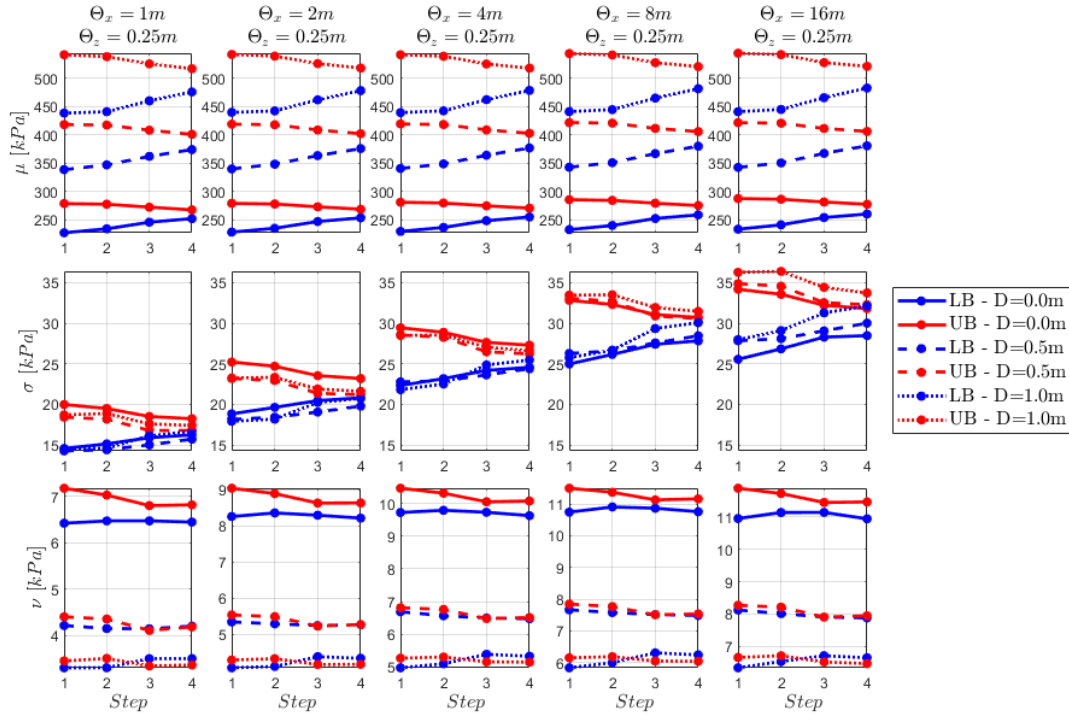
Figure 8: Diagrams of mean value, standard deviation and coefficient of variation of bearing capacities of a shallow foundation as a function of the step of adaptive mesh refinement procedure for vertical scale of fluctuation θ_z=1.0 m.

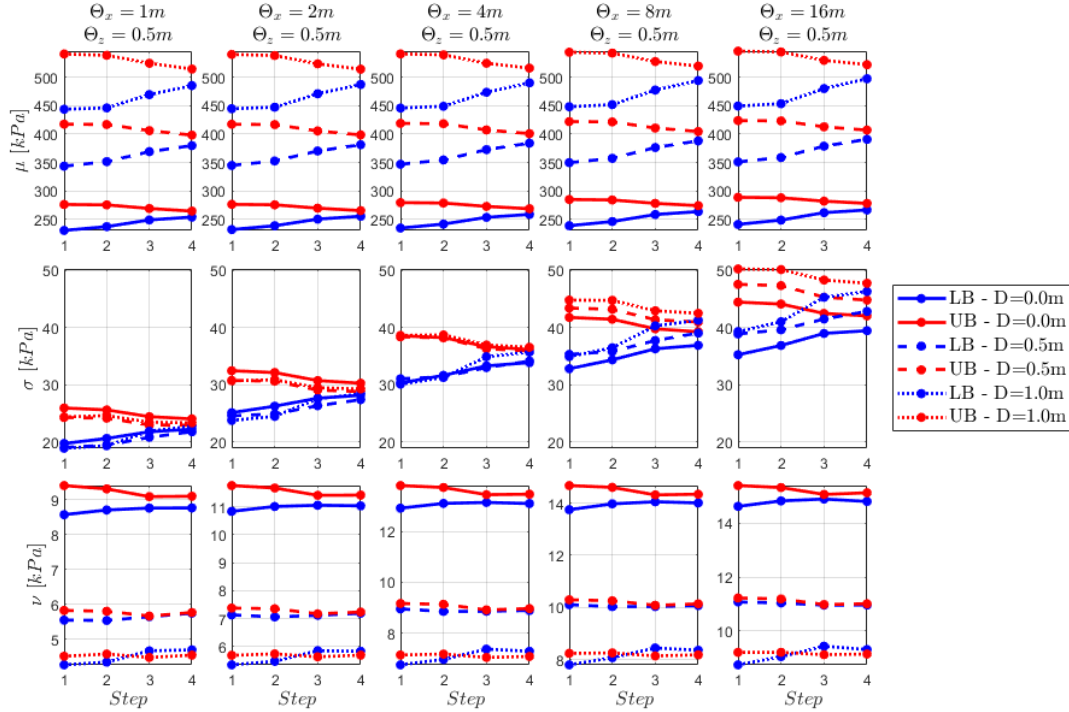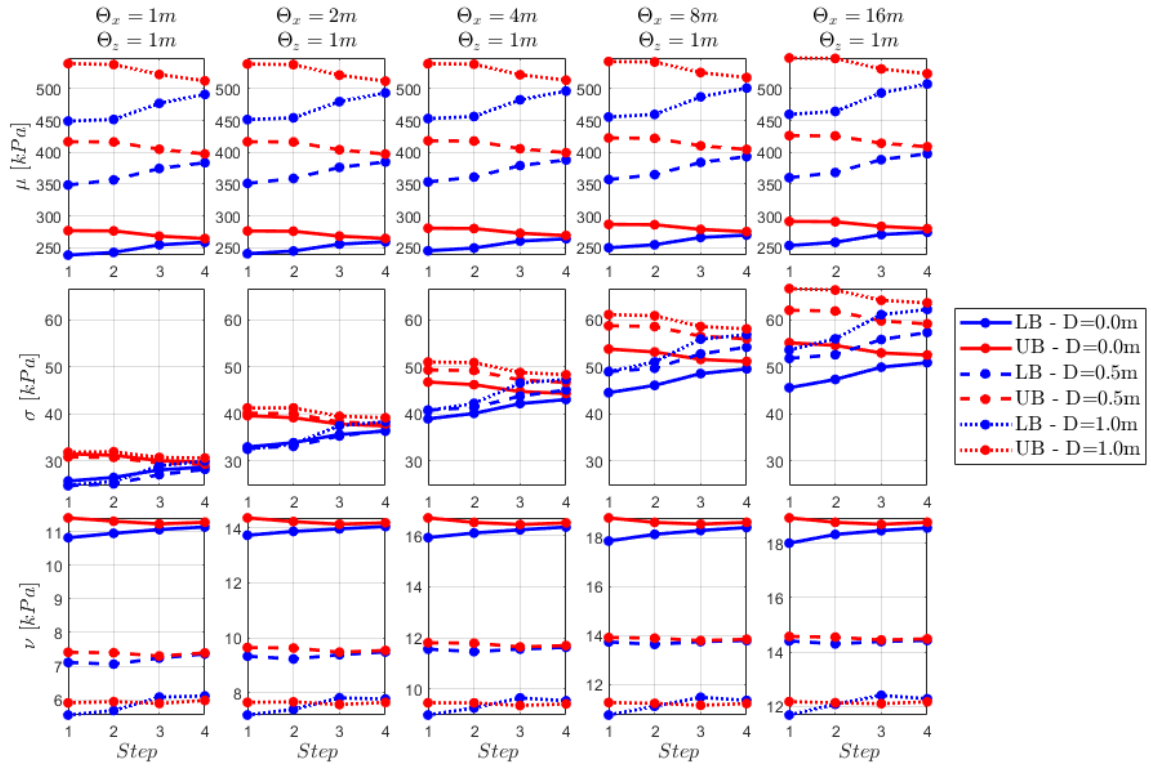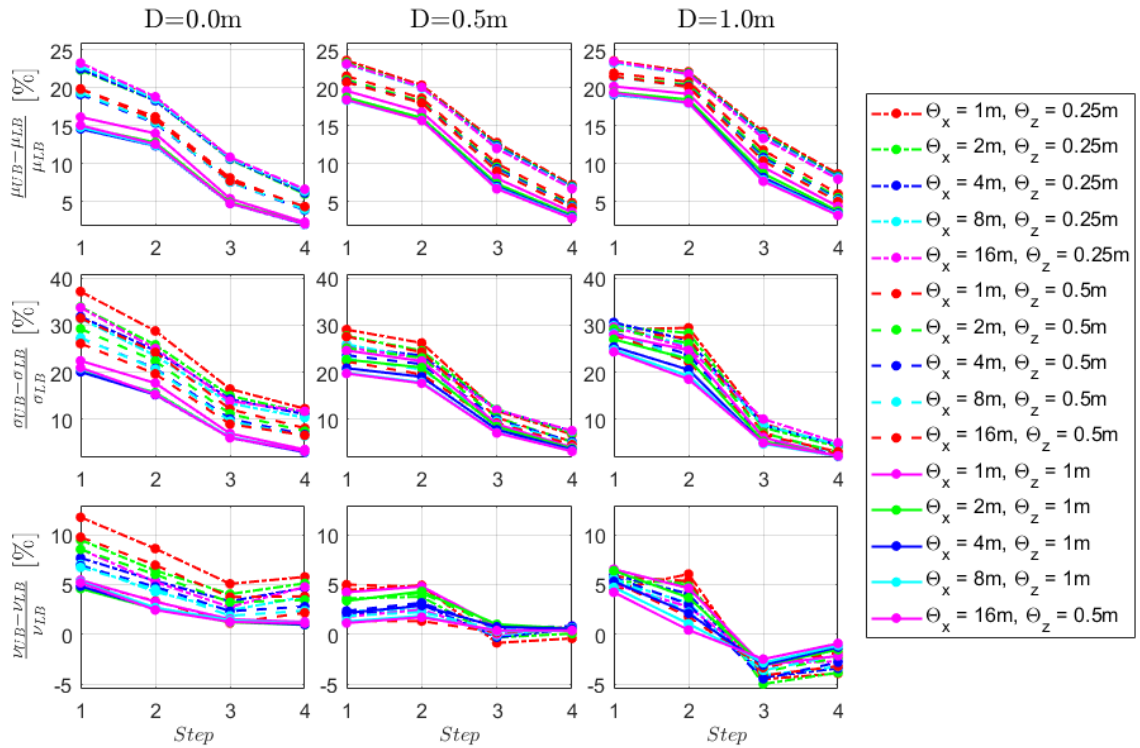**Figure 9**: Diagrams of the relative difference in mean, standard deviation and coefficient of variation between the upper and lower bound estimations as a function of following mesh adaptation procedure steps for all considered foundation levels.
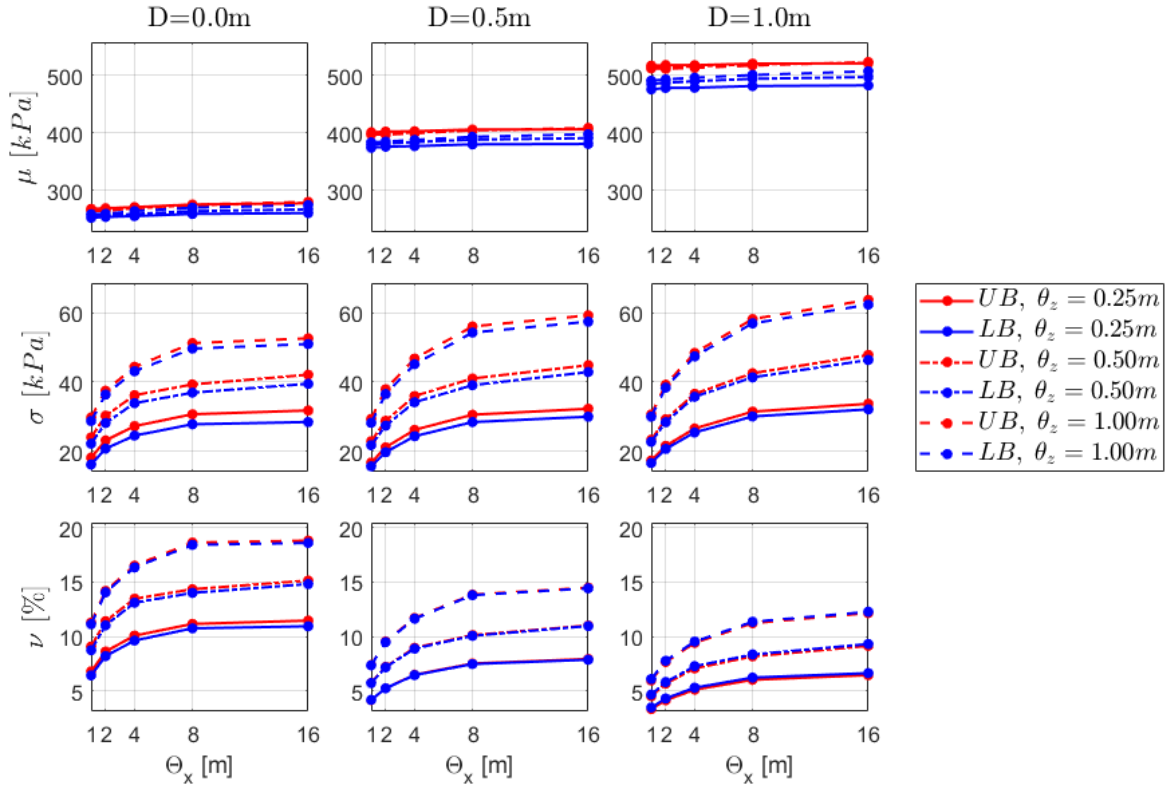
Figure 10: Diagrams of mean value, standard deviation and coefficient of variation as a function of the horizontal scales of fluctuations θ_x for all considered foundation levels and vertical scales of fluctuations θ_z.

scale (however, slight increase for greater scale value can be observed), although significantly dependent on the foundation level. However, the standard deviation is strongly related to the value of the horizontal fluctuation scale and the foundation level. This is caused by the magnitude of the failure mechanism that occurs when the yield criterion is reached. The greater the foundation level, the wider and deeper the failure mechanism will extend, which means that the soil parameters are averaged over a much wider area. However, the standard deviation for the only isotropic case considered, namely for the horizontal and vertical scales of fluctuation $\theta_x=\theta_z=1.0$ m, for each foundation depth, are very close to each other regardless of the foundation depth. As the value of the horizontal fluctuation scale increases, the values of the standard deviations increase with different rates. The greater the foundation depth, the greater the increase in the standard deviation for successive scales of fluctuation values. Still, since the increase in the mean value of the bearing capacity for the deeper foundation (regardless of fluctuations scale) is even greater, the resulting coefficients of variations for the deeper foundation present smaller values. The obtained trends are similar to the values obtained in other

studies (Pieczyńska-Kozłowska et al., 2015;, Kawa & Puła, 2020).

Tables 1, 2 and 3 contain the calculated values of the mean, standard deviation and coefficient of variation of the estimated limit-bearing capacities for D=0.0, 0.5 and 1.0 m, respectively.

3.1 Conservative estimation of the allowable load value

The results described in the previous chapter are based on 10,000 MCS realisations. By using RFELA for a single fluctuation scale, these amount of calculations were carried out in about 8–10 hours. It is worth noting that, although the lower estimation results always estimate the load conservatively, even such a large number of realisations do not allow a sufficiently accurate estimation of the probability of failure for the ultimate limit state of the foundation. According to EN-1990, for the standard 50-year reference period, the allowable reliability index should be greater than β=3.8 which corresponds to the failure probability lower than p_f=7.23•10^{-5}. According

Table 1*: The mean values, standard deviations and coefficients of variation for the lower and upper bound of bearing capacity estimated based on results from the last (fourth) step of the adaptive mesh procedure – D=0.0 m.*

Scales of fluctuations		Lower-bound estimation			Upper-bound estimation		
		Mean value (kPa)	Standard deviation (kPa)	Coefficient of variation (%)	Mean value (kPa)	Standard deviation (kPa)	Coefficient of variation (%)
θx =1.0 m	θz =0.25m	252.11	16.25	6.44	267.60	18.24	6.82
	θz =0.5 m	254.02	22.25	8.76	264.53	24.05	9.09
	θz =1.0 m	258.28	28.77	11.14	264.19	29.80	11.28
θx =2.0 m	θz =0.25 m	253.51	20.82	8.21	268.67	23.19	8.63
	θz =0.5 m	255.50	28.19	11.03	265.44	30.29	11.41
	θz =1.0 m	259.00	36.39	14.05	264.32	37.49	14.18
θx =4.0 m	θz =0.25 m	255.01	24.58	9.64	270.63	27.30	10.09
	θz =0.5 m	258.76	33.90	13.10	268.74	36.19	13.47
	θz =1.0 m	263.80	43.09	16.34	269.03	44.39	16.50
θx =8.0 m	θz =0.25 m	258.78	27.83	10.75	275.21	30.71	11.16
	θz =0.5 m	263.71	36.93	14.01	274.16	39.31	14.34
	θz =1.0 m	269.69	49.62	18.40	275.12	51.20	18.61
θx =16.0 m	θz =0.25 m	260.23	28.48	10.94	277.44	31.81	11.46
	θz =0.5 m	254.02	39.49	14.81	278.15	42.09	15.13
	θz =1.0 m	274.18	50.94	18.58	279.80	52.57	18.79

Table 2: The mean values, standard deviations and coefficients of variation for the lower and upper bound of bearing capacity estimated based on results from the last (fourth) step of the adaptive mesh procedure – D=0.5m.

Scales of fluctuations		Lower-bound estimation			Upper-bound estimation		
		Mean value (kPa)	Standard deviation (kPa)	Coefficient of variation (%)	Mean value (kPa)	Standard deviation (kPa)	Coefficient of variation (%)
θx =1.0 m	θz =0.25 m	374.15	15.73	4.20	401.09	16.79	4.19
	θz =0.5 m	379.86	21.81	5.74	398.32	22.95	5.76
	θz =1.0 m	383.55	28.25	7.36	397.40	29.39	7.39
θx =2.0 m	θz =0.25 m	375.96	19.79	5.26	402.26	21.20	5.27
	θz =0.5 m	381.39	27.42	7.19	398.58	28.83	7.23
	θz =1.0 m	384.83	36.53	9.49	397.09	37.92	9.55
θx =4.0 m	θz =0.25 m	376.99	24.40	6.47	403.00	26.23	6.51
	θz =0.5 m	384.16	34.17	8.90	400.92	35.96	8.97
	θz =1.0 m	387.88	45.13	11.64	399.40	46.74	11.70
θx =8.0 m	θz =0.25 m	380.13	28.46	7.49	405.97	30.59	7.53
	θz =0.5 m	388.19	39.09	10.07	404.65	41.01	10.14
	θz =1.0 m	393.19	54.23	13.79	404.47	56.00	13.85
θx =16.0 m	θz =0.25 m	380.82	30.02	7.88	406.25	32.29	7.95
	θz =0.5 m	390.91	42.87	10.97	407.12	44.85	11.02
	θz =1.0 m	397.74	57.36	14.42	408.76	59.19	14.48

Table 3: The mean values, standard deviations and coefficients of variation for the lower and upper bound of bearing capacity are estimated based on results from the last (fourth) step of the adaptive mesh procedure – D=1.0 m.

Scales of fluctuations		Lower-bound estimation			Upper-bound estimation		
		Mean value (kPa)	Standard deviation (kPa)	Coefficient of variation (%)	Mean value (kPa)	Standard deviation (kPa)	Coefficient of variation (%)
θx =1.0 m	θz =0.25 m	476.12	16.68	3.50	517.23	17.42	3.37
	θz =0.5 m	485.51	22.77	4.69	514.61	23.37	4.54
	θz =1.0 m	491.12	30.03	6.11	512.43	30.66	5.98
θx =2.0 m	θz =0.25 m	478.43	20.74	4.34	518.28	21.61	4.17
	θz =0.5 m	487.44	28.43	5.83	514.32	29.29	5.69
	θz =1.0 m	493.39	38.40	7.78	511.90	39.23	7.66
θx =4.0 m	θz =0.25 m	478.85	25.47	5.32	518.15	26.62	5.14
	θz =0.5 m	490.31	35.75	7.29	516.22	36.59	7.09
	θz =1.0 m	496.35	47.37	9.54	513.48	48.38	9.42
θx =8.0 m	θz =0.25 m	481.79	30.08	6.24	520.81	31.47	6.04
	θz =0.5 m	494.37	41.32	8.36	519.78	42.54	8.18
	θz =1.0 m	501.01	56.89	11.35	517.61	58.12	11.23
θx =16.0 m	θz =0.25 m	482.99	32.12	6.65	521.34	33.73	6.47
	θz =0.5 m	497.53	46.35	9.32	522.34	47.79	9.15
	θz =1.0 m	507.52	62.26	12.27	523.68	63.66	12.16

to Kolmogorov's inequality, 4,194,304 realisations are required to obtain a credible (with 95% confidence and a relative error of less than 10%) Monte-Carlo estimator of such a low probability (Kawa, 2023). Such a number of simulations is not feasible in a reasonable time. This number could be probably significantly reduced by using one of the variance reduction techniques, e.g., Subset Simulation (Au & Beck, 2001), but using such a method is out of the scope of the current work.

As mentioned above, as the consequence of the rigorousness of FELA, the results described above are consistently characterised by a lower mean value and lower standard deviation for LB bearing capacity estimations and greater mean and greater standard deviation for UB bearing capacity estimations. While this relationship is less intuitive in the case of standard deviation, it was clearly observed in all considered cases. It is important to note that the lower mean value of bearing capacity distribution with fixed standard deviation always lead to greater probability of ultimate limit state failure and thus conservative estimation of allowable load. On the other hand, an increase in the standard deviation of structural response results in an increased probability of failure, which in the consequence also lead to conservative

allowable load estimation. For this reason, adopting a distribution with a lower mean based on the results of the LB (static) approach and a higher standard deviation based on the UB (kinematic) approach appears to be a safe and conservative approximation of the probabilistic bearing capacity behaviour. Such a distribution with the following moments will be referred to as the mixed solution.

$$\mu=\min\{\mu_{LB},\mu_{UB}\}=\mu_{LB}$$
$$\sigma=\max\{\sigma_{LB},\sigma_{UB}\}=\sigma_{UB} \quad\quad (6)$$

Based on the distributions with values of mean and standard deviation presented above including upper-, lower- and mixed-approach distributions, the values of the reliability-based design loads for the analysed shallow foundations were estimated. By following the mentioned EN-1990 guidelines, p_f=7.23•10^{-5} (β=3.8) was assumed as an allowable probability condition. For a given distribution, the allowable reliability-based design load value can be obtained as:

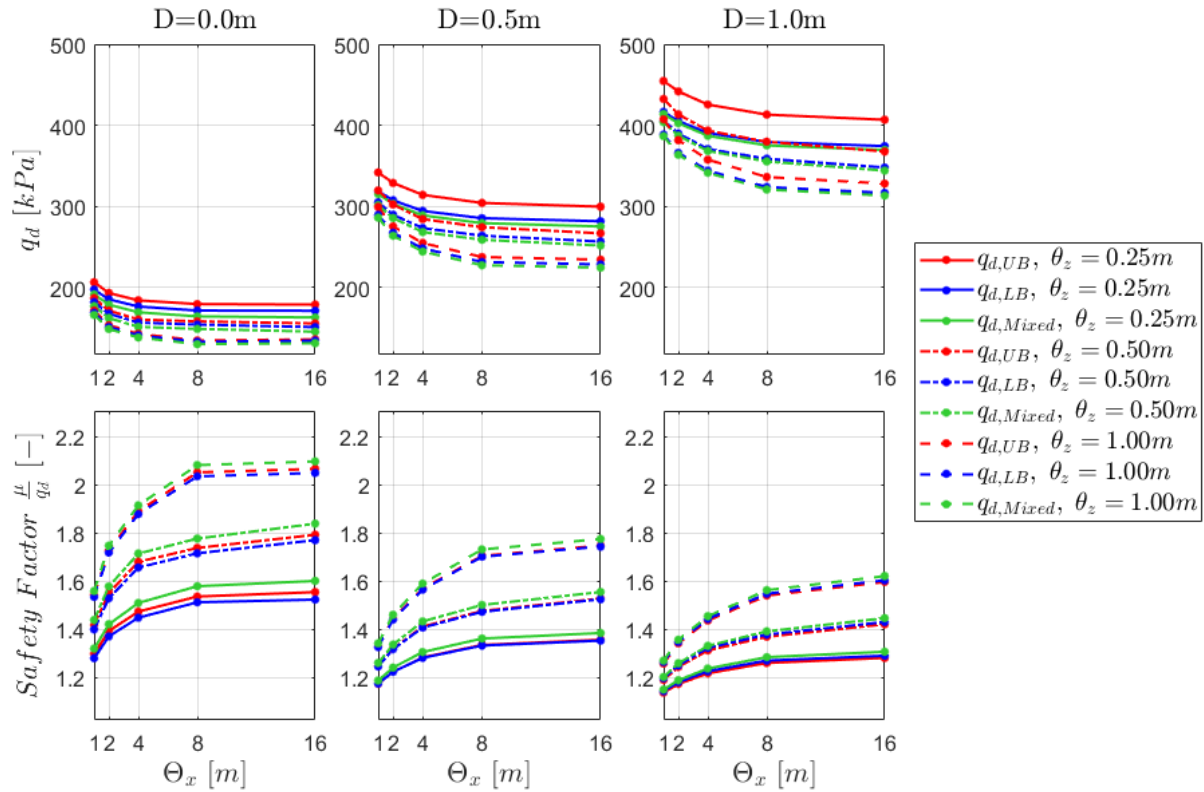$$q_d=\Phi^{-1}(p_f) \quad\quad (7)$$

Figure 11: Diagrams of allowable loads and safety factors as a function of the horizontal scales of fluctuations θ_x with a constant vertical scale of fluctuation for all considered foundation levels.

where Φ^1 denotes the inverse cumulative distribution function of the considered distribution

Figure 11 illustrates the results in the form of diagrams of the allowable load q_d and the safety factor, understood as the ratio of the mean value to the value of the allowable load. Both variables were plotted as a function of the horizontal scale of fluctuation. Subsequent vertical scales of fluctuation have been marked with solid, dash-dotted and dashed lines, respectively. Once again, results for different foundation levels are presented in different columns. The red colour represents the upper estimate, the blue the lower estimate and the green the mixed approach. As the horizontal scale of fluctuation increases, a decrease in the allowable load value of the foundation and an increase in the safety factor can be observed. The safety factor determines the reduction in the ultimate bearing capacity that must occur for the assumption of an acceptable probability of structural failure to be satisfied. For the same values of the fluctuation scales, increasing the foundation level from D=0.0 to 1.0 m means a decrease in the factor by 10%–25%. Again, the general trends are similar to the values obtained in other studies (Pieczyńska-Kozłowska et al., 2015;, Kawa & Puła, 2020).

The results from Figure 11 are also summarised in Tables 4, 5 and 6.

Please note that the approach utilising the distribution estimated based on the LB usually provides a lower (more conservative) estimate of the allowable load than the analogous approach based on the UB. However, since the rate of convergence differs between the LB, UB, mean and standard deviation, it may be possible that the LB results will estimate the mean value of the real solution better than the standard deviation. If such a standard deviation is too low, the allowable load distribution based on the LB may not be a conservative one. It should be noted that for the different scenarios, the mixed approach always provides a conservative and quite precise (as indicated by the small differences between the values provided by the different approaches) estimation. Moreover, this precision could be further improved (if the current precision level in the given problem is not satisfactory) by increasing the number of steps in the adaptive mesh refinement procedure. Since the moments of the upper and lower approaches can be accurately estimated even for lower numbers of realisations, the mixed approach provides a rigorous, conservative and effective approach

Table 4: Allowable loads for β=3.8 obtained for lower LB, upper UB and mixed approach estimated distributions – D=0.0 m.

Scales of fluctuations		Design value			Safety Factor		
Horizontal	Vertical	LB [kPa]	UB [kPa]	MIXED [kPa]	LB [-]	UB [-]	MIXED [-]
θ_x =1.0 m	θz =0.25 m	196.99	206.12	191.09	1.28	1.30	1.32
	θz =0.5 m	181.53	186.61	176.61	1.40	1.42	1.44
	θz =1.0 m	168.33	171.25	165.75	1.53	1.54	1.56
θx =2.0 m	θz =0.25 m	185.03	192.94	178.46	1.37	1.39	1.42
	θz =0.5 m	167.21	171.17	161.95	1.53	1.55	1.58
	θz =1.0 m	150.77	153.06	148.29	1.72	1.73	1.75
θx =4.0 m	θz =0.25 m	176.14	183.70	169.00	1.45	1.47	1.51
	θz =0.5 m	156.28	160.01	151.00	1.66	1.68	1.71
	θz =1.0 m	140.51	142.40	137.87	1.88	1.89	1.91
θx =8.0 m	θz =0.25 m	171.18	179.21	163.95	1.51	1.54	1.58
	θz =0.5 m	153.78	157.81	148.49	1.71	1.74	1.78
	θz =1.0 m	132.59	134.16	129.61	2.03	2.05	2.08
θx =16.0 m	θz =0.25 m	170.89	178.54	162.62	1.52	1.55	1.60
	θz =0.5 m	150.67	155.24	145.06	1.77	1.79	1.84
	θz =1.0 m	133.86	135.50	130.80	2.05	2.06	2.10

for reliability analysis. With these features, the proposed approach seems to be applicable in engineering practice.

3.2 Research significance

As has been mentioned in the introduction, the application of the FELA approach to the estimation of the bearing capacity of a shallow foundation has a recognisable history. However, until now, the rigorousness of this technique has not been fully exploited. The main motivation for writing this paper is to show a relatively simple application of this rigorousness for the conservative estimation of probability-based design values. As has been shown in the above section, such an application is possible.

It should be noted that the current study is subject to certain limitations. One of the most obvious is considering the structure in 2D as a plain strain problem. As a consequence, the value of the out-of-plane fluctuation scale was assumed to be infinite. The issue of modelling a problem of spatially variable soil, which is, in general, a 3D problem, in 2D space is well described in the literature for different issues (e.g., Liu et al. 2022). As shown in the paper (Chwała & Puła, 2020), omitting the fluctuation in out-of-plane direction can strongly influence the bearing capacity result by increasing the standard deviation of

the structure response. This means that 2D analysis of strip foundation based on random field lead to crude but conservatism estimation of bearing capacity probability distribution. A full 3D analysis of spatially variable soil was beyond the scope of the current work. However, we believe that the proposed method for estimating failure probability or allowable load values based on the mixed approach remains applicable to 3D analyses.

4 Conclusions

In the present work, probabilistic analysis of bearing capacity of strip foundation on spatially variable c - ϕ soil was performed. Variability of both strength parameters, i.e., cohesion c and angle of internal friction φ was described with lognormal stationary anisotropic random fields generated with FSM. The analysis included a few different values of horizontal and vertical fluctuation scales and different levels of foundation. The bearing capacity value was estimated using the FELA method with an adaptive mesh refinement procedure within the Monte-Carlo framework. For each problem (one pair of fluctuation scales and one foundation level), 10,000 simulations were computed. The results of the analysis

Table 5: Allowable loads for β=3.8 obtained for lower LB, upper UB and mixed approach estimated distributions – $D = 0.5\ m$.

Scales of fluctuations		Design value			Safety factor		
Horizontal	Vertical	LB [kPa]	UB [kPa]	MIXED [kPa]	LB [-]	UB [-]	MIXED [-]
θx =1.0 m	θz =0.25 m	318.66	341.82	315.19	1.17	1.17	1.19
	θz =0.5 m	304.96	319.53	301.46	1.25	1.25	1.26
	θz =1.0 m	289.25	299.34	285.95	1.33	1.33	1.34
θx =2.0 m	θz =0.25 m	307.40	328.85	303.02	1.22	1.22	1.24
	θz =0.5 m	289.56	302.10	285.45	1.32	1.32	1.34
	θz =1.0 m	267.29	275.22	263.59	1.44	1.44	1.46
θx =4.0 m	θz =0.25 m	294.26	314.12	288.81	1.28	1.28	1.31
	θz =0.5 m	273.07	284.18	268.20	1.41	1.41	1.43
	θz =1.0 m	247.97	254.68	244.02	1.56	1.57	1.59
θx =8.0 m	θz =0.25 m	285.32	304.16	279.22	1.33	1.33	1.36
	θz =0.5 m	263.68	274.16	258.67	1.47	1.48	1.50
	θz =1.0 m	231.18	237.32	227.17	1.70	1.70	1.73
θx =16.0 m	θz =0.25 m	281.51	299.53	275.09	1.35	1.36	1.38
	θz =0.5 m	256.46	266.60	251.48	1.52	1.53	1.55
	θz =1.0 m	228.21	234.00	224.17	1.74	1.75	1.77

Table 6: Allowable loads for β=3.8 obtained for lower LB, upper UB and mixed approach estimated distributions – $D = 1.0\ m$.

Scales of fluctuations		Design value			Safety factor		
Horizontal	Vertical	LB [kPa]	UB [kPa]	MIXED [kPa]	LB [-]	UB [-]	MIXED [-]
θx =1.0 m	θz =0.25 m	416.52	454.87	414.07	1.14	1.14	1.15
	θz =0.5 m	405.84	432.65	403.93	1.20	1.19	1.20
	θz =1.0 m	388.64	407.56	386.73	1.26	1.26	1.27
θx =2.0 m	θz =0.25 m	405.40	441.97	402.59	1.18	1.17	1.19
	θz =0.5 m	389.96	413.64	387.31	1.25	1.24	1.26
	θz =1.0 m	366.12	381.61	363.75	1.35	1.34	1.36
θx =4.0 m	θz =0.25 m	390.72	425.73	387.11	1.23	1.22	1.24
	θz =0.5 m	370.82	393.48	368.37	1.32	1.31	1.33
	θz =1.0 m	344.08	357.64	341.39	1.44	1.44	1.45
θx =8.0 m	θz =0.25 m	379.37	413.29	375.19	1.27	1.26	1.28
	θz =0.5 m	358.78	379.78	355.39	1.38	1.37	1.39
	θz =1.0 m	323.79	336.16	320.73	1.55	1.54	1.56
θx =16.0 m	θz =0.25 m	374.40	406.94	369.61	1.29	1.28	1.31
	θz =0.5 m	347.94	367.66	344.07	1.43	1.42	1.45
	θz =1.0 m	316.59	328.09	313.23	1.60	1.60	1.62

allowed to introduce mixed distribution with mean values based on lower and standard deviation on UBs which can be further used for efficient and conservative reliability analysis of the considered problem.

The following conclusions can be drawn from the paper:

– Foundations are parts of the structures associated with greater failure consequences than the other element. Meantime, they are the only parts of the structure in contact with strongly spatially variable soil. For this reason, this part of the structure might be recommended for reliability analysis. While the spatial variability of the foundation can be described with the random field, the complicacy of such description and, more importantly, the high computation cost of associated calculations are the main reasons that such analysis is not popular in engineering practice.

– The long computation time associated with probabilistic modelling of foundations is strongly associated with the assumed method for solving individual realisations of random fields. RFELA provides a much more effective way of solving problems with soil parameter variability modelled with random fields. While the class of tasks solved with this method is limited to the limit state problems, the foundation's ultimate limit state (bearing capacity) belongs to this category. Since the computation time benefits are significant the method seems to be of particular importance.

– The analysis performed in this paper focused on single-layer c - ϕ soil with both parameters defined as random fields. The influence of horizontal and vertical scales, and depth of foundation on estimated bearing capacity results were analysed. As shown, the mean value slightly increases and the standard deviation significantly increases with the scale of fluctuation. As a result, according to a simple reliability analysis performed based on estimated distributions the allowable load decreases and the factor of safety increases with the increasing scale of fluctuation. The effect is less significant for the greater depth of the foundation. Similar observation comes from other studies (Pieczyńska-Kozłowska et al., 2015; Kawa & Puła, 2020).

– The most important finding of the current work is introducing a mixed distribution with mean value based on LB estimation results and standard deviation based on UB estimation results. As shown the identification of the distribution moments is possible in reasonable time and the obtained distributions, using the rigorousness of FELA approaches, provide a conservative and precise estimate of allowable load. Due to these features, the proposed mixed approach with the moments obtained based, e.g., on a limited number of realisations obtained with FELA, seems to be an adequate candidate for a method possible to apply in engineering practice.

References

[1] Ali, A., Lyamin, A. V., Huang, J., Li, J. H., Cassidy, M. J., & Sloan, S. W. (2017). Probabilistic stability assessment using adaptive limit analysis and random fields. *Acta Geotechnica*, *12*(4), 937–948. https://doi.org/10.1007/s11440-016-0505-1

[2] Ali, A., Lyamin, A. V., Huang, J., Sloan, S. W., & Cassidy, M. (2016). Effect of Spatial Correlation Length on the Bearing Capacity of an Eccentrically Loaded Strip Footing. In H. W. Huang, J. Li, J. Zhang, & Chen J.B. (Eds.), *APSSRA*.

[3] Au, S.-K., & Beck, J. L. (2001). Estimation of small failure probabilities in high dimensions by subset simulation. *Probabilistic Engineering Mechanics*, *16*(4), 263–277. https://doi.org/10.1016/S0266-8920(01)00019-4

[4] Chen, X.-J., Fu, Y., & Liu, Y. (2022). Random finite element analysis on uplift bearing capacity and failure mechanisms of square plate anchors in spatially variable clay. *Engineering Geology*, *304*, 106677. https://doi.org/10.1016/j.enggeo.2022.106677

[5] Cheng, P., Guo, J., Yao, K., & Chen, X. (2023). Numerical investigation on pullout capacity of helical piles under combined loading in spatially random clay. *Marine Georesources & Geotechnology*, *41*(10), 1118–1131. https://doi.org/10.1080/1064119X.2022.2120843

[6] Ching, J., Wu, T. J., Stuedlein, A. W., & Bong, T. (2018). Estimating horizontal scale of fluctuation with limited CPT soundings. *Geoscience Frontiers*, *9*(6), 1597–1608. https://doi.org/10.1016/j.gsf.2017.11.008

[7] Chwała, M., Komatsu, G., & Haruyama, J. (2024). Structural stability of lunar lava tubes with consideration of variable cross-section geometry. *Icarus*, *411*. https://doi.org/10.1016/j.icarus.2023.115928

[8] Chwała, M., & Puła, W. (2020). Evaluation of shallow foundation bearing capacity in the case of a two-layered soil and spatial variability in soil strength parameters. PLoS One, 15(4), e0231992.

[9] Cho, S. E., & Park, H. C. (2010). Effect of spatial variability of cross-correlated soil properties on bearing capacity of strip footing. International Journal for Numerical and Analytical Methods in Geomechanics, 34(1), 1-26.

[10] Ciria Suárez, H. (2004). *Computation of Upper and Lower Bounds in Limit Analysis using Second-order Cone Programming and Mesh Adaptivity* [Master of Science]. Massachusetts Institute of Technology.

[11] Dobrzanski, J., & Kawa, M. (2021). Bearing capacity of eccentrically loaded strip footing on spatially variable cohesive soil. *Studia Geotechnica et Mechanica*, *43*(4), 425–437. https://doi.org/10.2478/sgem-2021-0035

[12] EN-1990, Basis of Structural Design. (2002).

[13] Engwirda, D. (2014). *Locally Optimal Delaunay-refinement and Optimisation-based Mesh Generation*.

[14] Fenton, G. A., & Griffiths, D. V. (2008). *Risk assessment in geotechnical engineering*. John Wiley & Sons.

[15] Griffiths, D. V., & Fenton, G. A. (1993). Seepage beneath water retaining structures founded on spatially random soil. *Géotechnique*, *43*(4), 577–587. https://doi.org/10.1680/geot.1993.43.4.577

[16] Griffiths, D. V., & Fenton, G. A. (2004). Probabilistic Slope Stability Analysis by Finite Elements. *Journal of Geotechnical and Geoenvironmental Engineering*, *130*(5), 507–518. https://doi.org/10.1061/(ASCE)1090-0241(2004)130:5(507)

[17] Griffiths, D. V., Huang, J., & Fenton, G. A. (2009). Influence of Spatial Variability on Slope Reliability Using 2-D Random Fields. *Journal of Geotechnical and Geoenvironmental Engineering*, *135*(10), 1367–1378. https://doi.org/10.1061/(ASCE)GT.1943-5606.0000099

[18] Hicks, M. A., & Samy, K. (2002). Influence of heterogeneity on undrained clay slope stability. *Quarterly Journal of Engineering Geology and Hydrogeology*, *35*(1), 41–49. https://doi.org/10.1144/qjegh.35.1.41

[19] Huang, L., Cheng, Y. M., Li, L., & Yu, S. (2021). Reliability and failure mechanism of a slope with non-stationarity and rotated transverse anisotropy in undrained soil strength. *Computers and Geotechnics*, *132*. https://doi.org/10.1016/j.compgeo.2020.103970

[20] *ISO 2394:2015, General principles on reliability for structures*. (2015).

[21] J. L. Doob. (1990). *Stochastic processes*. Wiley-Interscience.

[22] Jerez D. J. & Chwała M. & Jensen H. A. & Beer M. (2024). Optimal borehole placement for the design of rectangular shallow foundation systems under undrained soil conditions: A stochastic framework. Reliability Engineering & System Safety. doi.org/10.1016/j.ress.2023.109771.

[23] Jha, S. K., & Ching, J. (2013). Simulating Spatial Averages of Stationary Random Field Using the Fourier Series Method. *Journal of Engineering Mechanics*, *139*(5), 594–605. https://doi.org/10.1061/(ASCE)EM.1943-7889.0000517

[24] Kawa, M. (2023). *Zastosowania pól losowych do opisu anizotropowych ośrodków gruntowych w wybranych zagadnieniach geoinżynierii*. Oficyna Wydawnicza Politechniki Wrocławskiej (in Polish).

[25] Kawa, M., Baginska, I., & Wyjadlowski, M. (2019). Reliability analysis of sheet pile wall in spatially variable soil including CPTu test results. Archives of civil and mechanical engineering, 19, 598-613.

[26] Kawa, M., & Puła, W. (2020). 3D bearing capacity probabilistic analyses of footings on spatially variable c−φ soil. *Acta Geotechnica*, *15*(6), 1453–1466. https://doi.org/10.1007/s11440-019-00853-3

[27] Kawa, M., Puła, W., & Truty, A. (2021). Probabilistic analysis of the diaphragm wall using the hardening soil-small (HSs) model. *Engineering Structures*, *232*. https://doi.org/10.1016/j.engstruct.2021.111869

[28] Krabbenhoft, K., Lyamin, A. V., Hjiaj, M., & Sloan, S. W. (2005). A new discontinuous upper bound limit analysis formulation. *International Journal for Numerical Methods in Engineering*, *63*(7), 1069–1088. https://doi.org/10.1002/nme.1314

[29] Kumar, V., Burman, A., Portelinha, F. H. M., Kumar, M., Burman, A., Portelinha, F. H. M., & Das, G. (2023). Influence of Variation of Soil Properties in Bearing Capacity and Settlement Analysis of a Strip Footing Using Random Finite Element Method. *Civil Engineering Infrastructures Journal*. https://doi.org/DOI:10.22059/CEIJ.2023.360871.1930

[30] Liu, Y., Chen, X., & Hu, M. (2022). Three-dimensional large deformation modeling of landslides in spatially variable and strain-softening soils subjected to seismic loads. Canadian Geotechnical Journal, 60(4), 426-437.

[31] Liu, X., Wang, Y., & Li, D. Q. (2019). Investigation of slope failure mode evolution during large deformation in spatially variable soils by random limit equilibrium and material point methods. *Computers and Geotechnics*, *111*, 301–312. https://doi.org/10.1016/j.compgeo.2019.03.022

[32] Lyamin, A. V., & Sloan, S. W. (2002a). Lower bound limit analysis using non-linear programming. *International Journal for Numerical Methods in Engineering*, *55*(5), 573–611. https://doi.org/10.1002/nme.511

[33] Lyamin, A. V., & Sloan, S. W. (2002b). Upper bound limit analysis using linear finite elements and non-linear programming. *International Journal for Numerical and Analytical Methods in Geomechanics*, *26*(2), 181–216. https://doi.org/10.1002/nag.198

[34] Lyamin, A. V., & Sloan, S. W. (2003). Mesh generation for lower bound limit analysis. *Advances in Engineering Software*, *34*(6), 321–338. https://doi.org/10.1016/S0965-9978(03)00032-2

[35] Makrodimopoulos, A., & Martin, C. M. (2008). Upper bound limit analysis using discontinuous quadratic displacement fields. *Communications in Numerical Methods in Engineering*, *24*(11), 911–927. https://doi.org/10.1002/cnm.998

[36] Pieczyńska-Kozłowska, J. M., Puła, W., Griffiths, D. V., & Fenton, G. A. (2015). Influence of embedment, self-weight and anisotropy on bearing capacity reliability using the random finite element method. *Computers and Geotechnics*, *67*, 229–238. https://doi.org/10.1016/j.compgeo.2015.02.013

[37] Podlich, N. C. (2018). *The Development of Efficient Algorithms for Large-Scale Finite Element Limit Analysis* [Doctor of Philosophy]. University of Newcastle.

[38] Podlich, N. C., Lyamin, A. V., & Sloan, S. W. (2014). A Comparison of Conic Programming Software for Finite Element Limit Analysis. *Applied Mechanics and Materials*, *553*, 439–444. https://doi.org/10.4028/www.scientific.net/AMM.553.439

[39] Puła, W., Szabowicz, H., & Kawa, M. (2022). Efficient and conservative estimation of failure probability of strip footing on spatially variable soil using random finite element limit analysis. In J. Huang, D. V., Griffiths, S.-H. Jiang, A. Giacomini, & R. Kelly (Eds.), *8th International Symposiumon Geotechnical Safety and Risk (ISGSR)* (pp. 303–308). https://doi.org/10.3850/978-981-18-5182-7_04-007-cd

[40] Sert, S., Luo, Z., Xiao, J., Gong, W., & Juang, C. H. (2016). Probabilistic analysis of responses of cantilever wall-supported excavations in sands considering vertical spatial variability. *Computers and Geotechnics*, *75*, 182–191. https://doi.org/10.1016/j.compgeo.2016.02.004

[41] Simões, J. T., Neves, L. C., Antão, A. N., & Guerra, N. M. C. (2014). Probabilistic analysis of bearing capacity of shallow foundations using three-dimensional limit analyses. *International Journal of Computational Methods*, *11*(2). https://doi.org/10.1142/S0219876213420085

[42] Zaskórski, L., & Puła, W. (2016). Calibration of characteristic values of soil properties using the random finite element method. *Archives of Civil and Mechanical Engineering*, *16*(1), 112–124. https://doi.org/10.1016/j.acme.2015.09.007